Journal of Zhejiang University-SCIENCE A (Applied Physics & Engineering)
ISSN 1673-565X (Print); ISSN 1862-1775 (Online)
www.zju.edu.cn/jzus; www.springerlink.com
E-mail: jzus@zju.edu.cn

Sulphate attack resistance of high-performance concrete under compressive loading*

Hui XU[1], Yu-xi ZHAO[†‡1], Lei CUI[2], Bi XU[3]

([1]*Institute of Structural Engineering, Zhejiang University, Hangzhou 310058, China*)

([2]*School of Civil Engineering, Newcastle University, Newcastle upon Tyne NE1 7RU, UK*)

([3]*CCCC Tianjin Dredging Co., Ltd., Tianjin 300450, China*)

[†]E-mail: yxzhao@zju.edu.cn

Received Mar. 2, 2013; Revision accepted June 3, 2013; Crosschecked June 21, 2013

Abstract: In this paper, an experimental study on the sulphate attack resistance of high-performance concrete (HPC) with two different water-to-binder ratios (w/b) under compressive loading is presented. The sulphate concentration, compressive strength, and the mass change in the HPC specimens were determined for immersion in a Na_2SO_4 solution over different durations under external compressive loading by self-regulating loading equipment. The effects of the compressive stress, the w/b ratio, and the Na_2SO_4 solution concentration on the HPC sulphate attack resistance under compressive loading were analysed. The results showed that the HPC sulphate attack resistance under compressive loading was closely related to the stress level, the w/b ratio, and the Na_2SO_4 solution concentration. Applying a 0.3 stress ratio for the compressive loading or reducing the w/b ratio clearly improved the HPC sulphate attack resistance, whereas applying a 0.6 stress ratio for the compressive loading or exposing the HPC to a more concentrated Na_2SO_4 solution accelerated the sulphate attack and HPC deterioration.

Key words: Sulphate attack resistance, High-performance concrete (HPC), Compressive loading
doi:10.1631/jzus.A1300067 **Document code:** A **CLC number:** TU528

1 Introduction

Concrete structures in an underground environment are usually exposed to various chemical substances, including sulphate and chloride, which are ubiquitous in soil, groundwater and seawater and are damaging (Leemann and Loser, 2011). It has long been recognised that sulphate attack usually results in the formation of expansive products, such as ettringite, gypsum and thaumasite, which are produced by sulphate ions reacting with hydration products in cement, resulting in expansion, cracking, spalling, and concrete strength loss (Gonzáles and Irassar, 1997; Tian and Cohen, 2000; Baghabra Al-Amoudi, 2002; Collepardi, 2003; Neville, 2004; Idiart *et al.*, 2011). To improve concrete resistance to sulphate attack, many researchers have been developing high-performance concrete (HPC), which contains materials such as fly ash, silica fume, volcanic ash, natural pozzolan, fibers, and other materials, either separately or in various combinations (Park *et al*., 1999; Mbessa and Péra, 2001; Shannag and Shaia, 2003; Dawood and Ramli, 2012). The use of fly ash or silica fume has been reported as a highly effective treatment for reducing sulphate-induced damage or enhancing the sulphate resistance of cements (Torii *et al*., 1995; Lee *et al*., 2005; Sezer *et al*., 2008; Bonakdar and Mobasher, 2010). Reducing the concrete w/b ratio or adopting a suitable type of cement can also improve concrete resistance to sulphate attack (Monteiro and Kurtis, 2003; Kockal and Turker, 2007; Chen and Jiang, 2009).

Concrete structures in underground environments not only suffer from attack by chemical substances but

‡ Corresponding author

* Project supported by the National Natural Science Foundation of China (No. 50974107), and the Engineering Project of High School Subject Innovation (No. B07028), China

also from high stresses induced by underground water in the overlaying soil and surrounding rock that can lead to structural damage (Ahmad and Azhar, 2004; Yao *et al.*, 2007). This stress-induced damage can accelerate sulphate diffusion in concrete leading to concrete damage. Thus, the deterioration of concrete components from sulphate attack and external loads significantly affects the durability of underground concrete structures. Jin *et al.* (2008), Chen and Jiang (2009), and Gao *et al.* (2013) studied sulphate attack coupled to flexural loading and showed that the flexural load accelerated concrete deterioration; however, using a low water-to-binder (w/b) ratio or mixing approximately 20% fly ash into the concrete increased the concrete resistance. Bassuoni and Nehdi (2009) found that under the combined action of sulphate attack, cyclic environments and flexural stress, a high stress level of 50% caused the concrete to fail suddenly. Yang and Luo (2012) conducted an experimental study on the interaction between sulphate and chloride attack and mechanical loading on HPC using an ultrasonic technic: the flexural loading accelerated the HPC damage, whereas sulphate attack damage was mitigated in the presence of chlorides. However, few studies to date have considered the process of concrete damage from sulphate attack under compressive loading, which simulates the effects of the overlaying soil and surrounding rock on the underground concrete structure.

Therefore, this study probes the effect of coupling between sulphate and compressive loading on HPC sulphate attack resistance. To achieve this objective, 185 cubic HPC specimens with w/b ratios of 0.30 and 0.35 were cast and exposed to a sulphate solution; the specimens were also subjected to different external compressive loadings applied by self-regulating loading equipment. The sulphate ion concentrations in the specimens were measured using the chemical method of barium chloride titration. The HPC resistance to sulphate attack under compressive loading was determined in this study.

2 Experimental

2.1 Materials

A Chinese standard 52.5 R (II) Portland cement, which was supplied by the Xuzhou Cement Co., China, and was similar to the ASTM type I ordinary Portland cement, was used in this study. The Class F and Grade II fly ash used in this research was provided by the Tongshan Electricity Plant; the fly ash was in compliance with ASTM C618. The silica fume was manufactured by Shandong Minglan Ganister Sand Material Co., Ltd., China. River sand with a fineness modulus of 2.7 and limestone with a maximum size of 10 mm were used as aggregates. A polycarboxylic-acid-type superplasticiser was dosed to maintain the fresh concrete slump in the 150 to 200 mm range. The performance index of the cement and the chemical composition of the fly ash are shown in Tables 1 and 2, respectively.

2.2 Specimens

Five groups consisting of 37 concrete specimens each were produced. Of the five groups of concrete specimens, a relatively high w/b of 0.35 was used in four groups, and w/b=0.30 was used for the specimens in the fifth group. The proportions of the concrete mix are given in Table 3. All of the HPC specimens were cast as cubes with dimensions of 100 mm×100 mm×100 mm; the specimens were demoulded after 24 h and cured in a laboratory with a relative humidity of 95% and a temperature of (20±3) °C for 28 d. Each specimen was then sealed on five sides, leaving one side open for diffusion.

The 37 specimens in group 1 were immersed in a 0.1 g/ml sodium sulphate (Na_2SO_4) solution with no external applied load. All of the specimens in groups 2 and 5 were immersed in a 0.1 g/ml Na_2SO_4 solution, under compressive loading at a stress ratio of 0.3 applied on the surface (i.e., the 28-d compressive strength ratio for the applied load). The 37 specimens

Table 1 Cement performance

Soundness	Specific surface area (m^2/kg)	Setting time (h)		Compressive strength (MPa)		Flexural strength (MPa)	
		Initial	Final setting time	3 d	28 d	3 d	28 d
Criteria	>300	≥0.75	≤6.5	≥27.0	≥56.0	≥5.5	≥8.0

Table 2 Chemical composition of fly ash

Chemical composition						Loss	ASTM classification
SiO_2	Al_2O_3	Fe_2O_3	CaO	MgO	SO_3		
37%	23%	14%	23%	1.2%	0.07%	29%	Class F, Grade II

Table 3 Proportions of concrete mixture prepared

w/b	Water	Binder			Fine aggregate (kg/m^3)	Coarse aggregate (kg/m^3)	Superplasticizer (kg/m^3)	Cubic compressive strength (MPa)
		Cement	Fly ash	Silicon powder				
0.35	187	383	115	35	8.0	45	1057	45
0.30	172	412	124	37	8.6	62	1021	62

in group 3 were immersed in a 0.1 g/ml Na_2SO_4 solution, under compressive loading at a stress ratio of 0.6 applied on the surface. The 37 specimens in group 4 were immersed in a 5% (0.05 g/ml) Na_2SO_4 solution, under compressive loading at a stress ratio of 0.3 applied on the surface. Table 4 details the test conditions for the individual cases and the notations used to describe the tests. All of the tests were carried out at a room temperature of (20±3) °C. To ensure that the pH and the Na_2SO_4 solution concentration remained constant during the diffusion process, the solution in the tank was tested and adjusted once every month.

Table 4 Specific combinations and groups

Group	w/b	Na_2SO_4 (g/ml)	Stress ratio
1	0.35	0.1	0.0
2	0.35	0.1	0.3
3	0.35	0.1	0.6
4	0.35	0.05	0.3
5	0.30	0.1	0.3

Compressive loading was applied on the cubic specimens using self-regulating loading equipment to ensure that the sulphate attack was simultaneous with the mechanical loading on the specimen. The loading equipment primarily consisted of a 50-t screw jack, a counterforce frame, and a stress sensor. To ensure that the concrete specimen stress was uniform, two stiffness bearers were placed on the two surfaces in contact with the counterforce frame and pressure sensor (Fig. 1).

2.3 Testing method

Three parameters were investigated in this study: the sulphate concentration, the compressive strength, and the mass. Of the 37 specimens in each group, the sulphate concentrations were measured in 10 specimens for immersion times of 30 d, 90 d, 150 d, 210 d, and 270 d; the compressive strengths and masses were

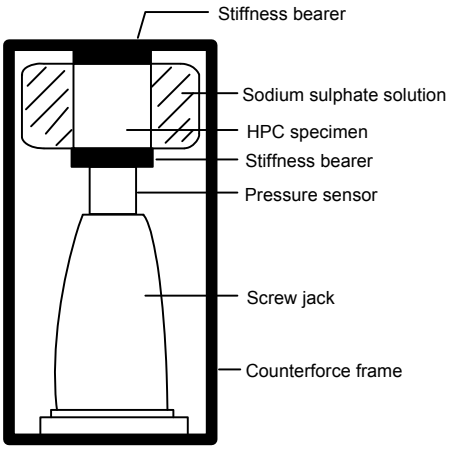

Fig. 1 Loading device

determined for the remaining 27 specimens for immersion times of 30 d, 60 d, 90 d, 120 d, 150 d, 180 d, 210 d, 240 d, and 270 d. All of the specimens in each group were air-dried for 30 min after immersion was completed, and the exposed surface of the dried specimens was cleaned with a steel wire brusher to completely remove salt crystals from the immersion test.

Concrete powder was collected from ten specimens in each group by drilling a 4-mm thick superficial zone. The powder from the concrete specimens was dried in an oven at 120 °C for 1 h and passed through a 0.63-mm sieve: the resulting powder samples were stored in airtight plastic bags (Sun *et al.*, 2013). Two specimens of the same immersion age were drilled to collect sufficient powder samples. The sulphate ion content of the powder samples was analysed using the barium sulphate gravimetric method (Detwiler *et al*., 2000).

Of the 27 specimens in each group, one group of three specimens was weighed using an electronic mass balance. The compressive strengths of the same specimens were then measured using an electrohydraulic servo tester: the average values of three measurements are presented in this study.

3 Results and discussion

3.1 Effect of compressive stress

3.1.1 Sulphate concentration

Fig. 2 shows the variation in the sulphate concentration with time for HPC specimens with a w/b ratio of 0.35, which were immersed in a 0.1 g/ml Na_2SO_4 solution for three different compressive loads. The results showed that the sulphate concentration of the specimens in all of the environments increased with the immersion time. Thus, sulphate diffused freely into the concrete from the external sulphate solution. For less than 90 d of immersion, the differences in the specimen sulphate concentrations among the three stress ratios for the compressive loading were small. This result can be explained by the simultaneity of calcium hydroxide dissolution and C-S-H decalcification with sulphate diffusion in concrete (Marchand *et al*., 2002), where the dissolution and decalcification dominated at early immersion times. However, after 270 d of corrosion, the highest sulphate concentration was observed for specimens under compressive loading with a stress ratio of 0.6, whereas the specimens under compressive loading at a 0.3 stress ratio exhibited the lowest sulphate concentrations. Thus, compressive loading at a 0.3 stress ratio prevented the ingress of sulphate into the concrete, whereas the sulphate diffusion rate increased after the stress ratio reached 0.6. This behaviour can be attributed to micro-cracks that are only generated and propagated beyond 0.6 stress levels. These results are in good agreement with the observations of Yu *et al*. (2012). A small external compressive loading caused extrusion of the HPC, which became denser, and thus the micro-structure was positively modified. However, cracks have been observed when a sustained load is applied to specimens, because the enlargement of the channels for sulphate diffusion into concrete increases the sulphate diffusion rate.

3.1.2 Compressive strength

Fig. 3 shows the variations in the cubic compressive strength with time for HPC specimens with a w/b ratio of 0.35, which were immersed in a 0.1 g/ml Na_2SO_4 solution and subjected to three different compressive loads. Table 5 presents the corresponding strength loss of the concrete for each immersion time. The strength loss was calculated as follows (Al-Dulaijan *et al*., 2003):

$$\text{Strength loss (\%)}=[(A-B)/A]\times 100\%, \quad (1)$$

where A is the compressive strength (in MPa) of the three specimens before exposure to the sulphate solution, and B is the average compressive strength (in MPa) of the three specimens after exposure to the sulphate solution.

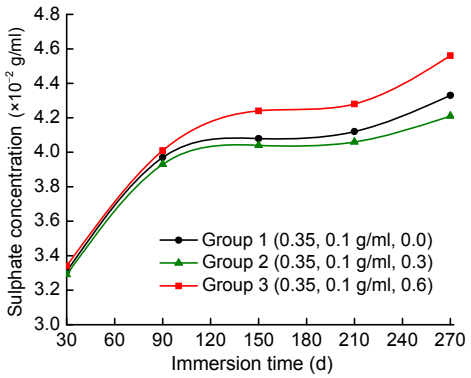

Fig. 2 Relationship between sulphate concentration and immersion time of HPC under different stress ratios

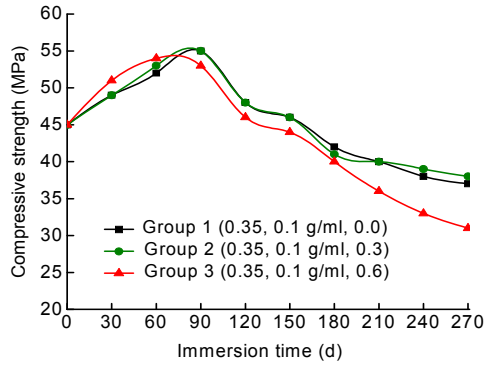

Fig. 3 Relationship between compressive strength and immersion time of HPC under different stress ratios

Fig. 3 clearly shows that the development of strength in HPC exposed to sulphate under compressive loading consisted of two stages, i.e., an initial increasing stage and a declining stage. This behaviour can be attributed to the transport of sulphate ions into the concrete pores where they reacted with hydration products to form expansive materials that blocked the pores, resulting in the development of micro-cracks and an interfacial transition zone at early immersion times; consequently, the HPC became more close-grained and the strength of the HPC specimens

Table 5 Strength loss of HPC with different stress ratios

Immersion condition	Strength loss (%)								
	30 d	60 d	90 d	120 d	150 d	180 d	210 d	240 d	270 d
Group 1 (0.35, 0.1 g/ml, 0.0)	−8.9	−15.6	−22.2	−6.7	−2.2	6.7	11.1	15.6	17.8
Group 2 (0.35, 0.1 g/ml, 0.3)	−8.9	−17.8	−22.2	−6.7	−2.2	8.9	11.1	13.3	15.6
Group 3 (0.35, 0.1 g/ml, 0.6)	−13.3	−20.0	−17.8	−2.2	2.2	11.1	20.0	26.7	31.1

increased. However, when the concrete pores cannot accommodate the material expansion, the concrete properties are negatively impacted. In particular, if the volume of the expansive material produced by the sulphate ions is much greater than the pore volume, internal expansion stresses can create both micro- and macro-cracks. Thus, the strength decreased in the late stages of the specimen immersion in the Na_2SO_4 solution. These results agreed with those of Wang *et al*. (2012).

The results for the specimens that were exposed to sulphate solutions under compressive loading with 0.3 stress ratios did not differ significantly from those for specimens exposed to Na_2SO_4 solutions only at early immersion times. The applied load was not very large and therefore did not have a significant effect on the compressive strength at the early immersion times. However, the specimens exposed to sulphate solutions under compressive loading at 0.3 stress ratios exhibited a lower strength loss (relative to the compressive strength for initial corrosion) after 270 d of immersion (15.6%), whereas the specimens that were only exposed to a sulphate solution exhibited a 17.8% strength loss. This result could be attributed to the small external compressive loading that made the HPC specimen more close-grained, thereby improving the long-term resistance of the HPC to sulphate attack. Note that at 180 d of immersion, the HPC specimens exposed to sulphate attack under compressive loading at a 0.3 stress ratio exhibited lower strengths than those exposed to a Na_2SO_4 solution only. This result may have been caused by experimental error and requires further validation.

The specimens exposed to Na_2SO_4 attack under compressive loading at a 0.6 stress ratio exhibited the highest compressive strengths during the early immersion times but the strengths decreased rapidly after 90 d of immersion. The largest strength loss of 31.1% was observed for 270 d of immersion. This result was attributed to the higher compressive stress that caused specimen extrusion, thereby enhancing the initial HPC pore structure; however, micro-cracks were generated and propagated through the specimens after a certain exposure period to sulphate, and combined with the sulphate attack action to rapidly deteriorate the concrete.

3.1.3 Concrete mass

Fig. 4 shows the variation in mass with time for HPC specimens with a w/b ratio of 0.35 immersed in a 0.1 g/ml Na_2SO_4 solution at three different compressive loads. The time-dependent mass curves consisted of two stages: an initial decreasing stage and an increasing stage. This behaviour implied that the calcium hydroxide dissolution rate exceeded the sulphate diffusion rate in the early immersion period, resulting in a decrease in the total mass. The sustained diffusion of Na_2SO_4 into the concrete weakened the calcium hydroxide dissolution; however, the sulphate ions reacted with the hydration products to form expansive products that filled the concrete pores, increasing the concrete mass density. Thus, the total specimen mass increased again during the late immersion stages.

Note that the largest masses of the HPC specimens exposed to sulphate attack under compressive loading at a 0.6 stress ratio were observed during the initial immersion period, whereas the next largest masses were exhibited by specimens exposed to sulphate attack under compressive loading at a 0.3 stress ratio and the smallest masses were exhibited by the specimens exposed to Na_2SO_4 only. However, following a period of immersion, the masses of the HPC specimens exposed to sulphate attack under compressive loading at a 0.6 stress ratio remained the largest, whereas the masses of the specimens exposed to sulphate under compressive loading at a 0.3 stress ratio were smaller than the masses of the specimens exposed to sulphate only. The effect of the stress ratios on the masses at the initial decreasing stage was probably caused by calcium hydroxide dissolution. The higher the stress ratio, the lower were the rates of calcium hydroxide and sulphate attack, and consequently, the

higher were the concrete masses. Calcium hydroxide dissolution decreased at later immersion times; however, crystallisation occurred in the interior and at the surface of the concrete exposed to these highly concentrated sulphate solutions, increasing the concrete mass. However, crystals dissolve as the environmental humidity changes (Rodriguez-Navarro *et al*., 2000). Thus, the change in the mass was low and the test results were indeterminate for the specimens under sustained loading at a 0.6 stress ratio. Loading at a 0.3 stress ratio was not sufficiently large to cause the HPC specimen to crack but enhanced the concrete pore structure. Thus, the HPC specimens exposed to sulphate under compressive loading at a 0.3 stress ratio exhibited the smallest masses in the increasing stage.

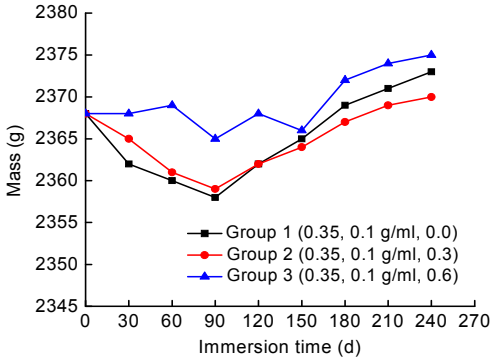

Fig. 4 Relationship between concrete mass and immersion time of HPC under different stress ratios

3.2 Effect of water-to-binder ratio

3.2.1 Sulphate concentration

Fig. 5 shows the variation in the sulphate concentration with time for HPC specimens with two w/b ratios, which were exposed to a 0.1 g/ml Na_2SO_4 solution under compressive loading at a 0.3 stress ratio. Fig. 5 clearly shows higher sulphate concentrations for HPC specimens with 0.35 w/b ratios than for those with 0.30 w/b ratios. Decreasing the w/b ratio reduced the concrete pore size, which is the key factor in determining the microstructure and penetrability of concrete. For HPC specimens exposed to sulphate under external compressive loading, the sulfate diffusion rate was sensitive to the water-binder ratio: the higher the water-to-cement ratio, the more rapidly could sulphate ions penetrate into the concrete. This behaviour can be explained in terms of the penetrability of the concrete depending mainly on the characteristics of the microstructure of the concrete. It was approved by the experimental results of Liang and Yuan (2004). The combined action of sulphate attack and an external load intensified the damage both in the initial and late stages under sustained loading; thus, the diffusion of sulphate ions from the Na_2SO_4 solution became more difficult.

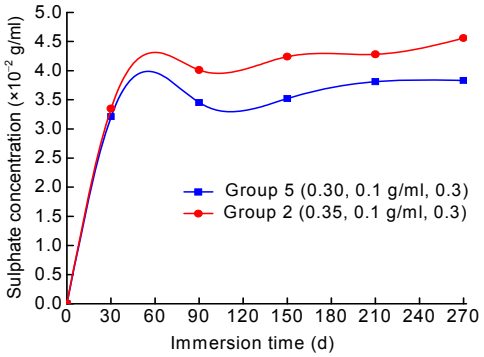

Fig. 5 Relationship between sulphate concentration and immersion time of HPC under different water-binder ratios

3.2.2 Compressive strength

Fig. 6 shows the variation in the compressive strength with time for HPC specimens at two w/b ratios, which were exposed to a 0.1 g/ml Na_2SO_4 solution under a compressive loading at a 0.3 stress ratio. Table 6 provides the corresponding strength losses for the concrete at each immersion time.

Fig. 6 shows that the w/b ratio affected the compressive strength of the specimens: the lower the w/b ratio of the concrete, the higher was the compressive strength, because reducing the concrete pore size made the microstructure denser (Lee *et al*., 2005). However, Table 6 clearly shows that although the actual strength of the low w/b specimens was higher than that of the high w/b specimens, the strength loss was higher for the high w/b specimens than the low w/b specimens. For example, for 270 d of immersion, the strength loss for the specimens with a w/b of 0.30 exposed to a 0.1 g/ml Na_2SO_4 solution under compressive loading at a 0.3 stress ratio was 31.1%, which was larger than the strength loss of 17.8% for specimens with a w/b ratio of 0.35. This result can be attributed to the higher cement content of specimens with lower w/b ratios, which resulted in the formation of more hydration products, thereby increasing the quantities of the reaction products ettringite and gypsum: therefore, the expansion pressure was observed earlier. Longer exposure times

are required to verify whether a similar trend is exhibited in the strength loss in the late stages of immersion.

3.2.3 Concrete mass

Fig. 7 shows the variations in the concrete mass with time for specimens with two w/b ratio exposed to a 0.1 g/ml Na_2SO_4 solution under compressive loading at a 0.3 stress ratio. Fig. 7 shows that the masses of the specimens with w/b ratios of 0.30 were larger than for those with w/b ratios of 0.35. This result can be explained by specimens with higher w/b ratios having larger mass densities and therefore higher masses. However, under combined sulphate immersion and external compressive loading, the increasing mass rate (relative to the mass from initial corrosion) of the specimens with 0.30 w/b ratios was higher than those with 0.35 w/b ratios. This result was obtained because the specimens with lower w/b ratios had higher cement contents, resulting in the formation of more hydration products and consequently higher quantities of sulphate ions and the reaction products, ettringite, and gypsum. Thus, the increasing mass rate of HPC specimens with lower w/b ratios was a little higher than for specimens with higher w/b ratios.

3.3 Effect of the immersion solution concentration

3.3.1 Sulphate concentration

Fig. 8 shows the variation in the sulphate concentration with time for HPC specimens with a w/b ratio of 0.35, which were exposed to Na_2SO_4 solutions (of 0.05 g/ml and 0.1 g/ml, respectively) under compressive loading at a 0.3 stress ratio. The curves in Fig. 8 show that under the same load conditions, the sulphate concentrations were much higher for HPC specimens exposed to a 0.1 g/ml Na_2SO_4 solution than those exposed to a 0.05 g/ml Na_2SO_4 solution. This result explains why the sulphate ion concentration in the HPC specimens exposed to sulphate under compressive loading was directly related to the concentration of the immersion sulphate solution: the higher the sulphate solution concentration, the more sulphate ions penetrated into the concrete. It is because sulphate ions enter concrete and diffuse through the pores from high concentration zone to low concentration. The high environmental sulphate concentration produced

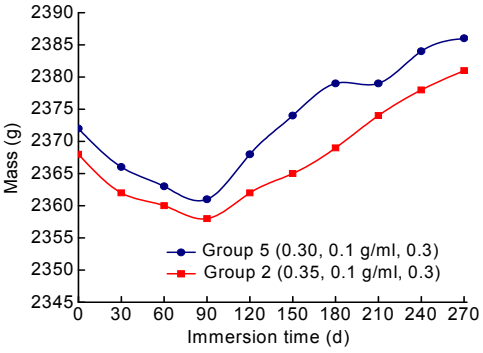

Fig. 7 Relationship between concrete mass and immersion time of HPC under different water-binder ratios

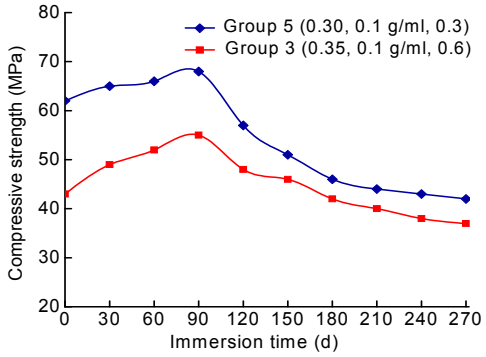

Fig. 6 Relationship between compressive strength and immersion time of HPC under different water-binder ratios

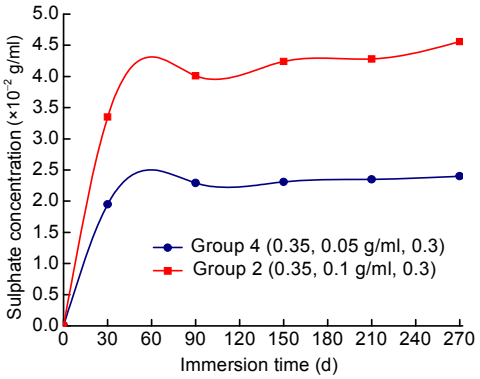

Fig. 8 Relationship between sulphate concentration and immersion time of HPC under different solution concentrations

Table 6 Strength loss of HPC with different water-binder ratios

Immersion condition	Strength loss (%)								
	30 d	60 d	90 d	120 d	150 d	180 d	210 d	240 d	270 d
Group 5 (0.30, 0.1 g/ml, 0.3)	−6.6	−8.2	−11.5	6.6	16.4	24.5	27.8	29.5	31.1
Group 2 (0.35, 0.1 g/ml, 0.3)	−8.9	−17.8	−22.2	−6.7	−2.2	8.9	11.1	13.3	15.6

the requisite concentration difference between the immersion solution and the concrete to increase the diffusion gradient, thereby accelerating sulphate diffusion into the HPC (Lorente *et al*., 2011). Furthermore, the ratio between the sulphate concentrations in the HPC specimens exposed to the 0.1 g/ml and 0.05 g/ml Na_2SO_4 solutions were between 1.70 and 2.00, which was similar to the ratio between the immersion sulphate concentrations.

3.3.2 Compressive strength

Fig. 9 shows the variation in the compressive strength with time for HPC specimens with a w/b ratio of 0.35 exposed to 0.1 g/ml and 0.05 g/ml Na_2SO_4 solutions under compressive loading at a 0.3 stress ratio. Table 7 provides the corresponding concrete strength losses at each immersion time.

Fig. 9 shows that under the same load condition, the compressive strength of the specimens exposed to a 0.1 g/ml Na_2SO_4 solution was higher than for those exposed to a 0.05 g/ml Na_2SO_4 solution at early immersion times; however, Table 7 shows a severe strength loss after 90 d of immersion. For instance, the strength loss for 270 d of immersion for specimens subjected to a 0.1 g/ml Na_2SO_4 solution under compressive loading at a 0.3 stress ratio was 17.8%, whereas the strength loss for specimens exposed to 0.05 g/ml Na_2SO_4 solution was only 4.4%. This observation can be explained by the positive effect of the sulphate attack on the compressive strength of the HPC specimens at early immersion times, as discussed in Section 3.1.2. At late immersion times, the sulphate attack negatively affected the compressive strength of the HPC specimens, because a higher Na_2SO_4 concentration in the solution produced more rapid expansion of the specimens, as has been reported by Santhanam *et al*. (2003); thus, an increase in the damage and the strength loss of the specimens was observed.

3.3.3 Concrete mass

Fig. 10 shows the variation in the concrete mass with time for HPC specimens with a w/b ratio of 0.35, which were exposed to 0.05 g/ml and 0.1 g/ml Na_2SO_4 solutions under compressive loading at a 0.3 stress ratio. Fig. 10 clearly shows that under the same load conditions, the specimen mass was higher for exposure to the 0.1 g/ml Na_2SO_4 solution than the 0.05 g/ml solution. This result was obtained because exposing concrete to higher sulphate concentrations formed more expansive products, which in turn increased the concrete mass. The mass curve of the specimens exposed to the 0.1 g/ml Na_2SO_4 solution was also steeper than that of the specimens exposed to the 0.05 g/ml Na_2SO_4 solution after 90-d immersion. This result showed that under the combined actions of sulphate attack and an external load, the concrete quality corresponding to the increasing rates was

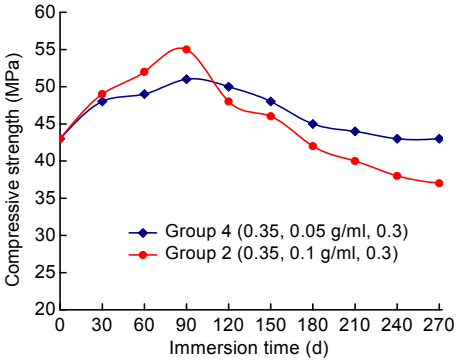

Fig. 9 Relationship between compressive strength and immersion time of HPC under different solution concentrations

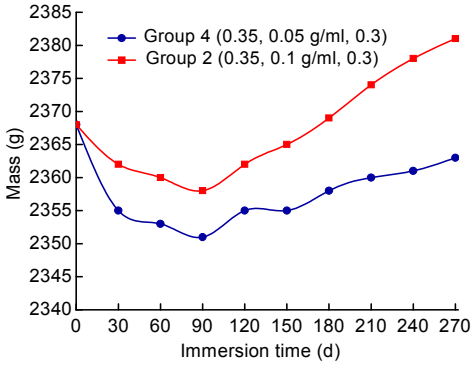

Fig. 10 Relationship between concrete mass and immersion time of HPC under different solution concentrations

Table 7 Strength loss of HPC with different immersion solution concentrations

Immersion condition	Strength loss (%)								
	30 d	60 d	90 d	120 d	150 d	180 d	210 d	240 d	270 d
Group 4 (0.35, 0.05 g/ml, 0.3)	−6.7	−8.9	13.3	−11.1	−4.4	0.0	2.2	4.4	4.4
Group 2 (0.35, 0.1 g/ml, 0.3)	−8.9	−17.8	−22.2	−6.7	−2.2	8.9	11.1	13.3	15.6

higher for HPC specimens exposed to higher Na_2SO_4 concentrations than for those exposed to lower Na_2SO_4 concentrations. It is because that the sustained load can increase the ion diffusion rate which was approved earlier by Francois *et al*. (1988). Longer exposure times are required to verify whether this trend persists at late immersion times.

4 Conclusions

In this paper, concrete specimens with two different w/b ratios that deteriorated under the combined action of sulphate immersion and compressive loading for 270 d were investigated. The sulphate concentration, the compressive strength, and the mass change in the HPC specimens were determined to evaluate the effects of the compressive stress, the w/b ratio, and the immersion solution concentration on the HPC resistance to sulphate attack. The conclusions drawn from this study are given below.

1. Exposing HPC to sulphate attack under compressive loading densified the concrete, thereby improving its initial resistance to sulphate attack.

2. The effect of external compressive loading on the resistance of HPC exposed to sulphate depended on the stress level: applying compressive loading at a 0.3 stress ratio clearly improved the sulphate attack resistance, whereas compressive loading at a 0.6 stress ratio accelerated the sulphate attack and the deterioration of the concrete.

3. Decreasing the w/b ratio improved the HPC resistance to sulphate attack under compressive loading, which could be explained in terms of the concrete pore size reduction, which filled up and densified the microstructure.

4. Increasing the environmental sulphate concentration accelerated the sulphate attack and HPC deterioration under the combined actions of sulphate attack and compressive loading.

References

Ahmad, I., Azhar, S., 2004. Temperature variation in high slump drilled shaft concrete and its effect on slump loss. *Cement and Concrete Research*, **34**(2):207-217. [doi:10.1016/S0008-8846(03)00257-6]

Al-Dulaijan, S.U., Maslehuddin, M., Al-Zahrani, M.M., Sharif, A.M., Shameem, M., Ibrahim, M., 2003. Sulfate resistance of plain and blended cements exposed to varying concentrations of sodium sulfate. *Cement and Concrete Composites*, **25**(4-5):429-437. [doi:10.1016/S0958-9465(02)00083-5]

Baghabra Al-Amoudi, O.S., 2002. Attack on plain and blended cements exposed to aggressive sulfate environments. *Cement and Concrete Composites*, **24**(3-4):305-316. [doi:10.1016/S0958-9465(01)00082-8]

Bassuoni, M.T., Nehdi, M.L., 2009. Durability of self-consolidating concrete to sulfate attack under combined cyclic environments and flexural loading. *Cement and Concrete Research*, **39**(3):206-226. [doi:10.1016/j.cemconres.2008.12.003]

Bonakdar, A., Mobasher, B., 2010. Multi-parameter study of external sulfate attack in blended cement materials. *Construction and Building Materials*, **24**(1):61-70. [doi:10.1016/j.conbuildmat.2009.08.009]

Chen, J., Jiang, M., 2009. Long-term evolution of delayed ettringite and gypsum in Portland cement mortars under sulfate erosion. *Construction and Building Materials*, **23**(2):812-816. [doi:10.1016/j.conbuildmat.2008.03.002]

Chen, S., Zheng, M., Wang, B.G., 2009. Study of high-performance concrete subjected to coupled action from sodium sulfate solution and alternating stresses. *Journal of Materials in Civil Engineering*, **21**(4):148-153. [doi:10.1061/(ASCE)0899-1561(2009)21:4(148)]

Collepardi, M., 2003. A state-of-the-art review on delayed ettringite attack on concrete. *Cement and Concrete Composites*, **25**(4-5):401-407. [doi:10.1016/S0958-9465(02)00080-X]

Dawood, E.T., Ramli, M., 2012. Durability of high strength flowing concrete with hybrid fibers. *Construction and Building Materials*, **35**:521-530. [doi:10.1016/j.conbuildmat.2012.04.085]

Detwiler, R., Taylor, P., Powers, L., 2000. Assessment of concrete in sulfate soils. *Journal of Performance of Constructed Facilities*, **14**(3):89-96. [doi:10.1061/(ASCE)0887-3828(2000)14:3(89)]

Francois, R., Maso, J.C., 1988. Effect of damage in reinforced concrete on carbonation or chloride penetration. *Cement and Concrete Research*, **18**(6):961-970. [doi:10.1016/0008-8846(88)90033-6]

Gao, J., Yu, Z., Song, L., Wang, T., Wei, S.W., 2013. Durability of concrete exposed to sulfate attack under flexural loading and drying-wetting cycles. *Construction and Building Materials*, **39**(7-9):33-38. [doi:10.1016/j.conbuildmat.2012.05.033]

Gonzáles, M.A., Irassar, E.F., 1997. Ettringite formation in low C_3A Portland cement exposed to sodium sulfate solution. *Cement and Concrete Research*, **27**(7):1061-1072. [doi:10.1016/S0008-8846(97)00093-8]

Idiart, A.E., López, C.M., Carol, G., 2011. Chemo-mechanical analysis of concrete cracking and degradation due to external sulfate attack: A meso-scale model. *Cement and Concrete Composites*, **33**(3):411-423. [doi:10.1016/j.cemconcomp.2010.12.001]

Jin, Z., Sun, W., Jiang, J., 2008. Damage of concrete attacked by sulfate and sustained loading. *Journal of Southeast University*, **24**(3):69-73.

Kockal, N.U., Turker, F., 2007. Effect of environmental

conditions on the properties of concretes with different cement types. *Construction and Building Materials*, **21**(3): 634-645. [doi:10.1016/j.conbuildmat.2005.12.004]

Lee, S.T., Moon, H.Y., Swamy, R.N., 2005. Sulfate attack and role of silica fume in resisting strength loss. *Cement and Concrete Composites*, **27**(1):65-76. [doi:10.1016/j.cemconcomp.2003.11.003]

Leemann, A., Loser, R., 2011. Analysis of concrete in a vertical ventilation shaft exposed to sulfate-containing groundwater for 45 years. *Cement and Concrete Composites*, **33**(1):74-83. [doi:10.1016/j.cemconcomp.2010.09.012]

Liang, Y.N., Yuan, Y.S., 2004. Detection of sulfate attacking on concrete with ultrasound. *Concrete*, **178**(8): 15-17 (in Chinese).

Lorente, S., Yssorche-Cubaynes, M., Auger, J., 2011. Sulfate transfer through concrete: Migration and diffusion results. *Cement & Concrete Composites*, **33**(7):735-741. [doi:10.1016/j.cemconcomp.2011.05.001]

Marchand, J., Samson, E., Maltais, Y., Beaudoin, J.J., 2002. Theoretical analysis of the effect of weak sodium sulfate solution on the durability of concrete. *Cement and Concrete Composites*, **24**(3-4):317-329. [doi:10.1016/S0958-9465(01)00083-X]

Mbessa, M., Péra, J., 2001. Durability of high-strength concrete in ammonium sulfate solution. *Cement and Concrete Research*, **31**(8):1227-1231. [doi:10.1016/S0008-8846(01)00553-1]

Monteiro, P.J.M., Kurtis, K.E., 2003. Time to failure for concrete exposed to severe sulfate attack. *Cement and Concrete Research*, **33**(7):987-993. [doi:10.1016/S0008-8846(02)01097-9]

Neville, A., 2004. The confused world of sulfate attack on concrete. Cement *and Concrete Research*, **34**(8):1275-1296. [doi:10.1016/j.cemconres.2004.04.004]

Park, Y.S., Soon, J.K., Lee, J.H., Shin, Y.S., 1999. Strength deterioration of high strength concrete in sulfate environment. *Cement and Concrete Research*, **29**(9):1397-1402. [doi:10.1016/S0008-8846(99)00106-4]

Rodriguez-Navarro, C., Doehne, E., Sebastian, E., 2000. How does sodium sulfate crystallize? Implications for the decay and testing of building materials. *Cement and Concrete Research*, **30**(10):1527-1534. [doi:10.1016/S0008-8846(00)00381-1]

Santhanam, M., Cohen, M.D., Olek, J., 2003. Effect of gypsum formation on the performance of cement mortars during external sulphate attack. *Cement and Concrete Research*, **33**(3):325-332. [doi:10.1016/S0008-8846(02)00955-9]

Sezer, G.İ., Ramyar, K., Karasu, B., Göktepe, B., Alper Sezer, A., 2008. Image analysis of sulfate attack on hardened cement paste. *Materials and Design*, **29**(1):224-231. [doi:10.1016/j.matdes.2006.12.006]

Shannag, M.J., Shaia, H.A., 2003. Sulfate resistance of high-performance concrete. *Cement and Concrete Composites*, **25**(3):363-369. [doi:10.1016/S0958-9465(02)00049-5]

Sun, C., Chen, J., Zhu, J., Zhang, M., Ye, J., 2013. A new diffusion model of sulfate ions in concrete. *Construction and Building Material*s, **39**(7-9):39-45. [doi:10.1016/j.conbuildmat.2012.05.022]

Tian, B., Cohen, M.D., 2000. Does gypsum formation during sulfate attack on concrete lead to expansion? *Cement and Concrete Research*, **30**(1):117-123. [doi:10.1016/S0008-8846(99)00211-2]

Torii, K., Taniguchi, K., Kawamura, M., 1995. Sulfate resistance of high fly ash content concrete. *Cement and Concrete Research*, **25**(4):759-768. [doi:10.1016/0008-8846(95)00066-L]

Wang, H.L., Dong, Y.S., Sun, X.Y., Jin, W.L., 2012. Damage mechanism of concrete deteriorated by sulfate attack in wet-dry cycle environment. *Journal of Zhejiang University* (*Engineering Science*), **46**(7):1255-1261 (in Chinese).

Yang, D., Luo, J., 2012. The damage of concrete under flexural loading and salt solution. *Construction and Building Materials*, **36**:129-134. [doi:10.1016/j.conbuildmat.2012.05.019]

Yao, Z., Cheng, H., Rong, C., 2007. Research on stress and strength of high strength reinforced concrete drilling shaft lining in thick top soils. *Journal of China University of Mining & Technology*, **17**(3):432-435. [doi:10.1016/S1006-1266(07)60120-5]

Yu, Z.X., Gao, J.M., Song, R.G., 2012. Damage process of concrete exposed to sulfate attack under drying-wetting cycles and loading. *Journal of Southeast University* (*Natural Science Edition*), **42**(3):487-491 (in Chinese).